Investigations of Monofluoro-Substituted Benzoates at the Tetradecyltrimethylammonium Micellar Interface†

ARTICLE *in* LANGMUIR · JANUARY 2002

Impact Factor: 4.46 · DOI: 10.1021/la0109765

4 AUTHORS, INCLUDING:

Martina Vermathen
Universität Bern
22 PUBLICATIONS **516** CITATIONS
SEE PROFILE

Ursula Simonis
San Francisco State University
46 PUBLICATIONS **842** CITATIONS
SEE PROFILE

Investigations of Monofluoro-Substituted Benzoates at the Tetradecyltrimethylammonium Micellar Interface†

M. Vermathen,‡ P. Stiles,‡ S. J. Bachofer,*,§ and U. Simonis*,‡

Department of Chemistry & Biochemistry, San Francisco State University, San Francisco, California 94132, and Department of Chemistry, Saint Mary's College of California, Moraga, California 94575

Received June 26, 2001. In Final Form: November 13, 2001

To shed more light on the factors that promote micelle growth and induce the sphere-to-rod transition, three micellar systems formed by surfactants containing tetradecyltrimethylammonium (TTA^+) as cation and *ortho*-, *meta*-, or *para*-fluorobenzoate as counterion were investigated by conductivity, surface tension, and ^1H, ^{19}F, and ^{13}C NMR spectroscopy. The investigations illustrate that the transfer of TTA^+/fluorobenzoate surfactants into the micellar phase and micelle growth are accompanied by characteristic changes in the NMR chemical shift and conductivity data, which were analyzed to determine the critical micelle concentration (cmc), the region of predominately spherical micelles, and the region of growth, where spherical aggregates are transformed to rodlike micelles. The studies reveal that TTA^+/*ortho*-fluorobenzoate micelles with an averaged cmc of 2.51 mM remain roughly spherical even at surfactant concentrations as high as 70 mM. The graphs, in which the specific conductivity is plotted versus increasing surfactant concentration or in which the chemical shifts of the *ortho*-fluorobenzoate or the TTA^+ resonances are plotted versus increasing or the inverse of increasing surfactant concentration, give rise to a single breakpoint at the onset of micellization. In contrast, the NMR and conductivity plots of TTA^+/*meta*- and *para*-fluorobenzoate micelles with averaged cmc values of 1.29 and 1.38 mM, respectively, show two breakpoints, one at the cmc and one at total surfactant concentrations 10 times the cmc. This second cmc indicates that TTA^+/*meta*- and *para*-fluorobenzoate micelles change shape and grow from roughly spherical to rodlike aggregates at higher surfactant concentration. The NMR data reveal that aggregate growth is not an abrupt but a rather continuous process and that the positioning of the benzoate ions at the micellar interface along with their reduction of headgroup repulsions are the major contributors to micelle growth. The *meta*- and *para*-fluorobenzoates intercalate among the $^+N(CH_3)_3$ headgroups thereby forming tight ion pairs, reducing headgroup repulsions, and inducing growth. Contrary, the *ortho*-fluorobenzoate ions penetrate the micellar interface more deeply and move toward the palisade layer. This positioning does not enable the anions to reduce effectively the unfavorable electrostatic headgroup interactions, and as a result, TTA^+/*ortho*-fluorobenzoate micelles remain spherical even at high surfactant concentrations.

Introduction

Cationic micelles with bound organic anions have received considerable attention in the chemical and biological industries.[1−6] Some of these systems transform from spherical to rodlike micelles, which upon entanglement exhibit remarkable properties, such as viscoelasticity,[7−14] streaming birefringence,[15,16] and drag reduction.[11,16−18] Surfactants known to form rodlike aggregates include cetyltrimethylammonium (CTA^+),[8−15,19−26] tetradecyltrimethylammonium (TTA^+),[12,27,28] and alkyl-

* To whom correspondence should be addressed. Dr. Ursula Simonis, Department of Chemistry & Biochemistry, San Francisco State University, 1600 Holloway Ave., San Francisco, CA 94132. Tel: (415) 338-1656. Fax: (415) 338-2384. E-mail: uschi@sfsu.edu. Dr. Steven J. Bachofer, Department of Chemistry, Saint Mary's College of California, P.O. Box 4527, Moraga, CA 94575. Tel: (925) 631-4694. Fax: (925) 376-4027. E-mail: bachofer@stmarys-ca.edu.

† Parts of the research described in this paper were presented as an invited talk at the Symposium of "Associate Colloids as Living Polymers" at the 216th National American Chemical Society Meeting in Boston, August 1998.

‡ San Francisco State University.

§ Saint Mary's College of California.

(1) Jones, M. N.; Chapman, D. *Micelles, Monolayers, and Biomembranes*; Wiley-Liss: New York, 1995.

(2) (a) Fendler, J. H.; Gilbert, R. D.; Yen, T. F. *Advances in the Applications of Membrane-Mimetic Chemistry*; Plenum Press: New York, 1995. (b) Cross, J.; Singer, E. J. *Cationic Surfactants*: *Analytical and Biological Evaluation*; Marcel Dekker: New York, 1994.

(3) Evans, D. F.; Wennerström, H. *The Colloidal Domain − Where Physics, Chemistry, and Biology Meet*, 2nd ed.; Wiley-VCH: New York, 1999.

(4) Rathman, J. F. *Curr. Opin. Colloid Interface. Sci.* **1996**, *1* (4), 514−518.

(5) Hiemenz, P. C.; Rajagopalan, R. *Principles of Colloid and Surface Chemistry*, 3rd ed.; Marcel Dekker: New York, 1997.

(6) Bunton, C. A.; Nome, F.; Quina, F. H.; Romsted, L. S. *Acc. Chem. Res.* **1991**, *24*, 357−364.

(7) Olsson, U.; Söderman, O.; Guéring, P. *J. Phys. Chem.* **1986**, *90*, 5223−5232.

(8) Gravsholt, S. *J. Colloid Interface Sci.* **1976**, *57*, 575−577.

(9) Iyer, R. M.; Rao, U. R. K.; Manohar, C.; Valauikar, B. S. *J. Phys. Chem.* **1987**, *91*, 3286−3291.

(10) Bachofer, S. J.; Turbitt, R. M. *J. Colloid Interface Sci.* **1990**, *135*, 325−334.

(11) Hoffmann, H.; Rehage, H.; Reizlein, K.; Thurn, H. In *Macro- and Microemulsions*: *Theory and Applications*; Shah, D. O., Ed.; ACS Symposium Series Vol. 272; American Chemical Society: Washington, DC, 1985; p 41−66.

(12) Ohlendorf, D.; Interthal, W.; Hoffmann, H. *Rheol. Acta* **1986**, *25*, 468−486.

(13) Hirata, H.; Shikata, T.; Kotaka, T. *Langmuir* **1988**, *4*, 354−359.

(14) Anet, F. A. L. *J. Am. Chem. Soc.* **1986**, *108*, 7102−7103.

(15) Ulmius, J.; Wennerström, H.; Johansson, L. B.-A.; Lindblom, G.; Gravsholt, S. *J. Phys. Chem.* **1979**, *83*, 2232−2236.

(16) Hoffmann, H.; Platz, G.; Rehage, H.; Schorr, W.; Ulbricht, W. *Ber. Bunsen-Ges. Phys. Chem.* **1981**, *85*, 255−266.

(17) Smith, B. C.; Chou, L. C.; Zakin, J. L. *J. Rheol.* **1994**, *38*, 73−83.

(18) Lu, B.; Li, X.; Scriven, L. E.; Davis, H. T.; Talmon, Y.; Zakin, J. L. *Langmuir* **1998**, *14*, 8−16.

(19) Magid, L. J.; Han, Z.; Warr, G. G.; Cassidy, M. A.; Butler, P. D.; Hamilton, W. A. *J. Phys. Chem. B* **1997**, *101*, 7919−7927.

(20) Kreke, P. J.; Magid, L. J.; Gee, J. C. *Langmuir* **1996**, *12*, 699−705.

(21) Carver, M.; Smith, T. L.; Gee, J. C.; Delichere, A.; Caponetti, E.; Magid, L. J. *Langmuir* **1996**, *12*, 691−698.

(22) Lin, M. Y.; Hanley, H. J. M.; Sinha, S. K.; Straty, G. C.; Peiffer, D. G.; Kim, M. W. *Phys. Rev. A* **1996**, *53* (5), R4302−R4305.

10.1021/la0109765 CCC: $22.00
Published on Web 01/26/2002

pyridiniumcations[29] comicellized with small organic counterions.[8−30] Benzoates, such as hydroxy- and chlorobenzoates, and tosylate,[8−29] belong to the group of anions that are known to influence micelle morphology, and TTA^+/ or CTA^+/benzoates are studied with great interest to probe micelle structure, dynamics, and growth.[17−35] Among the hydroxybenzoates, salicylate is most effective in forming rod-shaped micelles with alkylammonium surfactants in that growth is induced at low surfactant and anion concentrations.[7−9,11−15,33,36,37] Aggregates with *meta*-hydroxybenzoates as counterions grow only for specific surfactants,[9,17,29] whereas *para*-hydroxybenzoates[17,26,29] do not promote rodlike micelle formation independent of the nature and concentration of the surfactant. In contrast, surfactants comicellized with *para*- and *meta*-chlorobenzoates yield rods shortly after the onset of micellization, while CTA^+/*ortho*-chlorobenzoate micelles remain roughly spherical even at 60 mM surfactant concentrations.[9,17−21]

Comparing the behavior of chloro- and hydroxybenzoate aggregates, it is evident that the nature of both the counterion and the surfactant affect micelle size and shape. In regard to the aromatic counterion, it is discussed that its substitution pattern and the nature of its substituent,[19−21,29] its size,[29a] its hydrophobicity,[8,12,17,29a] and its degree of hydration[29b] determine its preferred location and orientation within or at the cationic micellar interface, which in turn is recognized to influence aggregate growth.[19−21,34,35] With respect to the surfactant, changes in concentration,[20,21] headgroup area,[28,35] charge density,[19] and electrostatic interactions among the headgroups[7,9,29c,35−38] are described to affect micelle morphology, which was formally discussed in terms of packing constraints of the aggregate.[38−43] Clearly, many factors influence micelle structure and shape. However, their relative importance in promoting aggregate growth is not well comprehended, and the understanding of the sphere-to-rod transition and the regime of growth remains, therefore, an area of active study in colloidal chemistry research.[11−26,35]

To probe micelle morphology changes, research groups,[13−15,20,29,40−47] including our laboratories,[10,27,28] have turned to NMR spectroscopy. Parameters such as chemical shifts,[20,21,27−29] chemical shift anisotropy,[43] relaxation rates,[42] or self-diffusion[43,46,48] are analyzed to investigate how counterions induce structural changes, to determine the average location and orientation of the anions at the cationic micellar interface in relationship to aggregate growth, and to characterize micelle size and shape. It is known that the incorporation of benzoates into TTA^+ or CTA^+ micelles gives rise to characteristic shielding and deshielding effects for the ^1H, ^{13}C, and ^{19}F nuclei of the anion and/or the surfactant as the surfactant concentration is increased.[9,10,17−20,27−30,43−47] Upon micellization, the ^1H signals of the benzoate ion shift both upfield and downfield. Upfield shifts are reported to imply the incorporation of a given proton in the micelle, whereas downfield shifts are interpreted to indicate increased proton−headgroup interactions.[20,27,28,43] The magnitudes of these shifts have been analyzed to determine the depths at which the anion penetrates the cationic micellar interface.[22,28,41] Two different explanations are given for the surfactant chemical shift trends. The protons of the surfactant headgroup region [$^+N(CH_3)_3$, α-, β-, and γ-CH_2] become shielded and move upfield upon increase in aggregate concentration, a trend which is opposite to that observed for the TTA^+/bromide (TTAB) surfactant alone.[49] These upfield shifts are attributed to magnetic anisotropy effects of the benzoate interacting with the surfactant molecules and are used to determine the anions' average location and orientation at the micellar interface.[20,30,44,50] On the other hand, chemical shift trends of the ^{13}C surfactant resonances have been interpreted by conformational changes that surfactants undergo when forming micelles.[45] Downfield shifts have been related to an increase in the number of trans conformers, whereas upfield shifts seem to indicate the increasing probability of gauche conformers.[45]

As noted above, chemical shift studies provide valuable information on micelle morphology changes. However, only a few spectral parameters including resonance line broadening have been identified as indicators of growth.[15,29a,44] Our interest in identifying spectral markers for the transformation of spherical to rodlike micelles and in determining how the nature of the counterion affects growth has led us to investigate micelles formed by the TTA^+ cation and *ortho*-, *meta*-, or *para*-fluorobenzoate as counterion. The investigations presented below reveal that TTA^+/fluorobenzoates are attractive systems for these studies. Micelles derived from these surfactants grow only at relatively high concentrations. Thus, a large surfactant

(23) (a) Soltero, J. F. A.; Puig, J. E.; Manero, O.; Schulz, P. C. *Langmuir* **1995**, *11*, 3337−3346. (b) Soltero, J. F. A.; Puig, J. E.; Manero, O. *Langmuir* **1996**, *12*, 2654−2662. (c) Soltero, J. F. A.; Puig, J. E.; Bautista, F.; Manero, O. *Langmuir* **1999**, *15*, 1604−1612.
(24) Hassan, P. A.; Valaulikar, B. S.; Manohar, C.; Kern, F.; Bourdieu, L.; Candau, S. J. *Langmuir* **1996**, *12*, 4350−4357.
(25) Salkar, R. A.; Hassan, P. A.; Samant, S. D.; Valaulikar, B. S.; Kumar, V. V.; Kern, F.; Candau, S. J.; Manohar, C. *J. Chem. Soc., Chem. Commun.* **1996**, 1223−1224.
(26) Johnson, I.; Olofsson, G. *J. Colloid Interface Sci.* **1985**, *106*, 222−225.
(27) Bachofer, S. J.; Simonis, U. *Langmuir* **1996**, *12*, 1744−1754.
(28) Bachofer, S. J.; Simonis, U.; Nowicki, T. A. *J. Phys. Chem.* **1991**, *95*, 480−488.
(29) (a) Bijma, K.; Engberts, J. B. F. N. *Langmuir* **1997**, *13*, 4843−4849. (b) Bijma, K.; Blandamer, M. J.; Engberts, J. B. F. N. *Langmuir* **1998**, *14*, 79−83. (c) Buwalda, R. T.; Stuart, M. C. A.; Engberts, J. B. F. N. *Langmuir* **2000**, *16*, 6780−6786.
(30) (a) Bacalogu, R.; Bunton, C. A.; Cerichelli, G.; Ortega, F. *J. Phys. Chem.* **1989**, *93*, 1490−1497. (b) Bunton, C.; Minch, M. J. *J. Phys. Chem.* **1974**, *78* (15), 1490−1498.
(31) Jansson, M.; Jönnsson, M. *J. Phys. Chem.* **1989**, *93*, 1451−1457.
(32) Kalus, J.; Hoffmann, H.; Ibel, K. *Colloid Polym. Sci.* **1989**, *267*, 818−824.
(33) Kim, W. J.; Yang, S. M.; Kim, M. *J. Colloid Interface Sci.* **1997**, *194*, 108−119.
(34) Imae, T.; Kohsaka, T. *J. Phys. Chem.* **1992**, *96*, 10030−10035.
(35) Magid, L. J. *J. Phys. Chem. B* **1998**, *102*, 4064−4074.
(36) Underwood, A. L.; Anacker, E. W. *J. Phys. Chem.* **1984**, *88*, 2390−2393.
(37) Underwood, A. L.; Anacker, E. W. *J. Colloid. Interface Sci.* **1985**, *106*, 86−93.
(38) (a) Rao, U. R. K.; Manohar, C.; Valaulikar, B. S.; Iyer, R. M. *J. Phys. Chem.* **1987**, *91*, 3286−3291. (b) Manohar, C.; Rao, U. R. K.; Valaulikar, B. S.; Iyer, R. M. *J. Chem. Soc., Chem. Commun.* **1986**, 379−381.
(39) Israelachvili, J. N.; Mitchell, D.; Ninham, B. W. *J. Chem. Soc., Faraday Trans. 2* **1976**, *72*, 1525−1567.
(40) (a) Zhao, J.; Fung, B. M. *J. Phys. Chem.* **1993**, *97*, 5185−5187. (b) May, S.; Ben-Shaul, A. *J. Phys. Chem. B* **2001**, *105*, 630−640.
(41) Kolehmainen, E. *Magn. Reson. Chem.* **1988**, *26*, 764−768.
(42) (a) Romsted, L. S.; Yoon, C. O. *J. Am. Chem. Soc.* **1993**, *115*, 989−994. (b) Soldi, V.; Keiper, J.; Romsted, L. S.; Ciccovia, I.; Chaimovich, H. *Langmuir* **2000**, *16*, 59−71.
(43) Lindman, B.; Olsson, U. *Ber. Bunsen-Ges. Phys. Chem.* **1996**, *100*, 344−363.
(44) Okano, L. T.; El Seoud, O. A.; Halstead, T. K. *Colloid Polym. Sci.* **1997**, *275*, 138−145.
(45) MacInnis, J. A.; Palepu, R.; Maragoni, D. G. *Can. J. Chem.* **2000**, *77*, 1994−2000.
(46) Chachaty, C. *Prog. Nucl. Magn. Reson. Spectrosc.* **1987**, *19*, 183−221.
(47) Lindman, B.; Olsson, U.; Söderman, O. *Dynamics of Solutions and Fluid Mixtures by NMR*; Delpuech, J.-J., Ed.; John Wiley & Sons Ltd: New York, 1995.
(48) (a) Söderman, O.; Stilbs, P. *Prog. Nucl. Magn. Reson. Spectrosc.* **1994**, *26* (5), 445−482. (b) Bjorling, M.; Herslof-Bjorling, A.; Stilbs, P. *Macromolecules* **1995**, *28* (20), 6970−6975. (c) Morris, K. F.; Johnson, C. S.; Wong, T. C. *J. Phys. Chem.* **1994**, *98*, 603−608.
(49) Vermathen, M.; Simonis, U. Manuscript in preparation.
(50) Stilbs, P. *J. Colloid Interface Sci.* **1983**, *94*, 463−469.

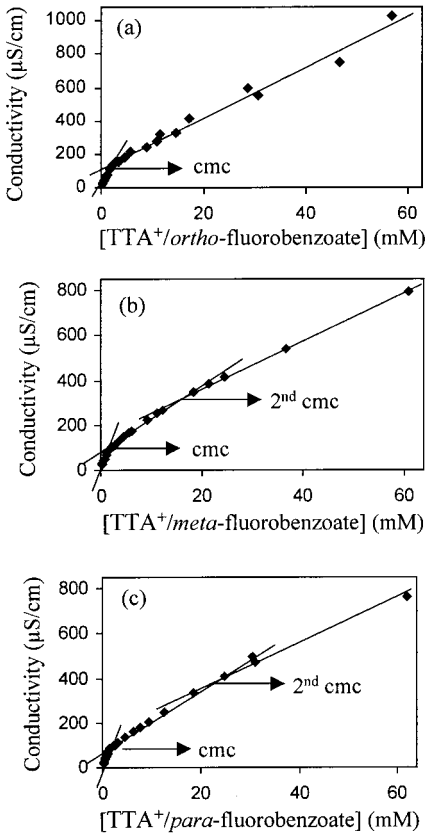

Figure 1. Graphs of the specific conductivities versus surfactant concentrations at 298 K of (a) 0.94−70.0 mM TTA^+/*ortho*-fluorobenzoate, (b) 0.60−60.0 mM TTA^+/*meta*-fluorobenzoate, and (c) 0.80−60.0 mM TTA^+/*para*-fluorobenzoate. The cmc and the second cmc values were determined from the intersections of the regression lines as is shown in each of the figures.

concentration range is provided, over which the transformation from surfactant monomers to spherical micelles to rodlike aggregates can be monitored. The data demonstrate that TTA^+/*ortho*-fluorobenzoate micelles remain spherical over the entire concentration range studied, while TTA^+/*meta*- and *para*-fluorobenzoates are gradually transformed from spherical to rodlike aggregates at concentrations around 10 times the critical micelle concentration (cmc). In agreement with conclusions drawn by other laboratories for related systems,[29c,35,40,51] our results highlight that micelle growth is a gradual process and that the most important contributor to growth is the ability of the benzoate anion to reduce headgroup repulsions, thereby lowering the curvature of the micelle and inducing growth.

Results and Discussion

In the search for markers to probe growth from spherical to rodlike micelles, three systems derived from TTA^+/*ortho*-, *meta*-, and *para*-fluorobenzoate surfactants were studied by surface tension, specific conductivity, and ^1H and ^{19}F NMR spectroscopy. For TTA^+/*ortho*- and *meta*-fluorobenzoate, ^{13}C NMR investigations were also carried out. Graphs, in which the specific conductance of all micellar systems is plotted versus increasing TTA^+/fluorobenzoate concentrations, are given in Figure 1. The chemical shifts of the aromatic ion and surfactant proton

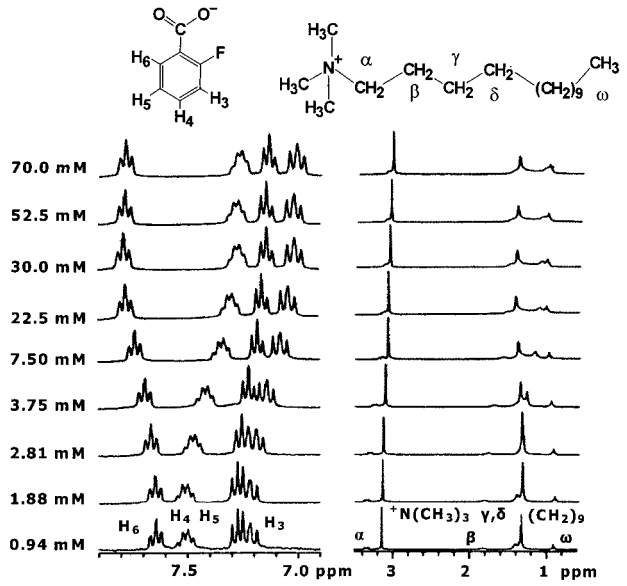

Figure 2. ^1H NMR spectra of 0.94−70.0 mM TTA^+/*ortho*-fluorobenzoate with the benzoate resonances plotted to the left and the TTA^+ resonances to the right. The two spectra at the bottom are recorded below the cmc, whereas all other spectra are recorded above the cmc. The ^1H signals are labeled according to the nomenclature typically employed for such systems using the labeling shown in the schematic structures of the *ortho*-fluorobenzoate anion and the TTA^+ cation.

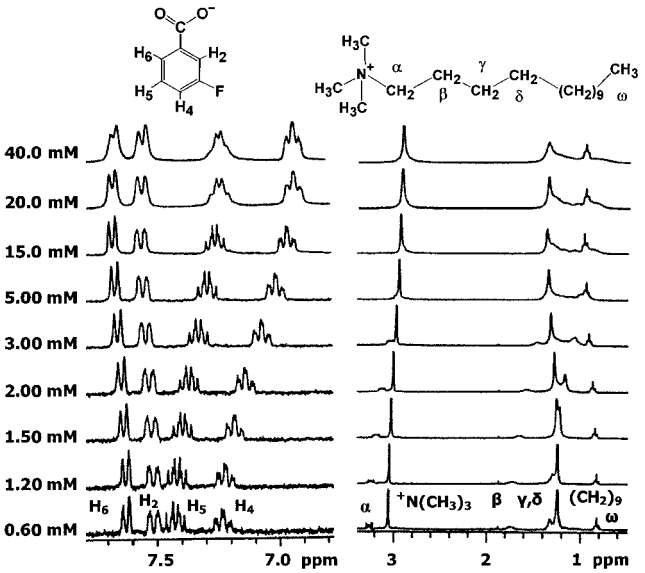

Figure 3. ^1H NMR spectra of 0.60−40.0 mM TTA^+/*meta*-fluorobenzoate. The benzoate resonances are plotted to the left, and the TTA^+ resonances, to the right. The two spectra at the bottom are recorded below the cmc, and the third spectrum is recorded close to the cmc, whereas all other spectra are recorded above the cmc. The signals are labeled according to the nomenclature typically employed for such systems using the labeling of the protons shown in the schematic structures of the *meta*-fluorobenzoate anion and the TTA^+ cation.

resonances with increasing TTA^+/fluorobenzoate concentrations are plotted in Figures 2−4, which also include the schematic structures of the fluorobenzoate anions and the TTA^+ cation with the labeling of the proton and carbon positions typically employed for such systems. Example plots of the ^1H chemical shifts of the anions versus increasing TTA^+/fluorobenzoate concentrations or the inverse of increasing TTA^+/fluorobenzoate concentrations are given in Figures 5 and 6. The ^1H NMR spectra were

(51) Bertrand, G. L.; Lindemuth, P. M. *J. Phys. Chem.* **1993**, *97*, 7769−7773.

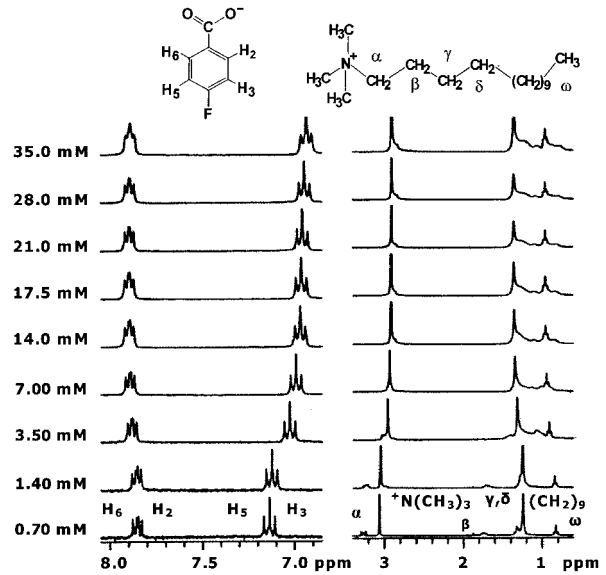

Figure 4. ^{1}H NMR spectra of 0.70−35.0 mM TTA$^+$/*para*-fluorobenzoate. The benzoate resonances are plotted to the left, and the TTA$^+$ resonances, to the right. The two spectra at the bottom are recorded below the cmc, whereas all other spectra are recorded above the cmc. The signals are labeled according to the nomenclature typically employed for such systems using the labeling shown in the schematic structures of the *para*-fluorobenzoate anion and the TTA$^+$ cation.

assigned unambiguously by one-dimensional ^{1}H−^{19}F decoupling and two-dimensional pulsed field gradient homonuclear correlation spectroscopy (PFG COSY) experiments. The ^{19}F-decoupled ^{1}H spectra of all micellar systems and the PFG COSY maps of TTA$^+$/*ortho*- and *meta*-fluorobenzoates are included in the Supporting Information (Figures S1 and S2, respectively). The ^{1}H−^{13}C coupling framework and the ^{13}C resonance assignments were established through the acquisition of heteronuclear ^{1}H−^{13}C correlation (HETCOR) and multiple bond correlation (HMQC) maps (not shown), which were also used to confirm the ^{1}H resonance assignments.

As is discussed in more detail below, the conductivity and NMR graphs provide complementary information and reveal significant differences between the three micellar systems. For TTA$^+$/*ortho*-fluorobenzoate, these plots (Figures 1a, 5a, and 6a) show two linear regimes over the total surfactant concentration range studied with a single breakpoint at the cmc. In the first regime below the cmc, the physical and spectroscopic properties are determined by the presence of predominately TTA$^+$/fluorobenzoate monomers in equilibrium with most likely premicellar aggregates. In the second regime above the cmc, they are governed by the equilibrium between surfactant monomers and spherical micelles that become the dominant contributors at higher surfactant concentrations. For TTA$^+$/*meta*- and *para*-fluorobenzoate micelles, an additional third regime with a second breakpoint at the onset of rodlike micelles is observed (Figures 1b,c, 5b,c, and 6b,c) at total surfactant concentrations 10 times the cmc, which is characterized by the gradual transformation from spherical to rodlike micelles.

Micelle Formation: cmc Values. The cmc values of all three TTA$^+$/fluorobenzoate surfactants (Table 1) were determined by (i) surface tension from the Gibb's absorption isotherm plots; (ii) conductivity measurements from the intersections of the two linear regression lines in the conductivity plots in the concentration range up to 10 times the cmc[52] (Figure 1); and (iii) ^{1}H NMR spectroscopy from the graphs, in which the surfactant or fluorobenzoate chemical shifts are plotted versus the inverse of increasing surfactant concentration (Figure 5) or increasing surfactant concentration (Figure 6) as is exemplified for TTA$^+$/*meta*-fluorobenzoate in Figure S3 (Supporting Information). The conductivity, the inverse,[45,53] and the chemical shift plots give rise to two straight lines in the concentration range of 0.6−10, 0.8−15, and 0.9−70 mM for TTA$^+$/*meta*-fluorobenzoate, TTA$^+$/*para*-fluorobenzoate, and TTA$^+$/*ortho*-fluorobenzoate, respectively, with intersections at the cmc or the inverse of the cmc. Micelle formation at the cmc is signaled in the spectra by an abrupt change in the TTA$^+$ and the benzoate ^{1}H chemical shifts (Figures 2−4). Below the cmc, the ^{1}H resonances shift only minimally with increasing TTA$^+$/fluorobenzoate concentrations. The

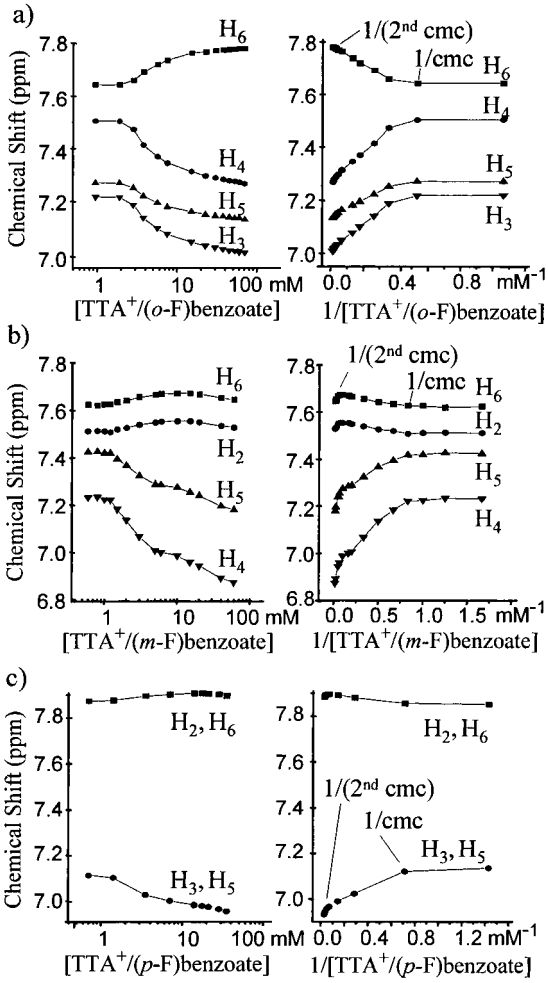

Figure 5. Plots of the benzoate proton chemical shifts versus increasing TTA$^+$/fluorobenzoate concentration (left side of the figure) or versus the inverse of increasing TTA$^+$/fluorobenzoate concentration (right side of the figure) for (a) TTA$^+$/*ortho*-fluorobenzoate, (b) TTA$^+$/*meta*-fluorobenzoate, and (c) TTA$^+$/*para*-fluorobenzoate. The cmc and the second cmc values were most conveniently determined from the regression lines in the inverse plots. Note that the TTA$^+$/fluorobenzoate concentration axes in the spectra to the left in each figure are drawn to clearly show that the signals for H_6 and H_2 for TTA$^+$/*meta*- and *para*-fluorobenzoate (left spectra in parts b and c, respectively) move at first downfield and reverse direction to move upfield at the second cmc as is shown more clearly in Figure 6.

(52) Treiner, C.; Makayssi, A. *Langmuir* **1992**, *8*, 794−800.
(53) Persson, B. O.; Drakenberg, T.; Lindman, B. *J. Phys. Chem.* **1979**, *83* (23), 3011−3015.

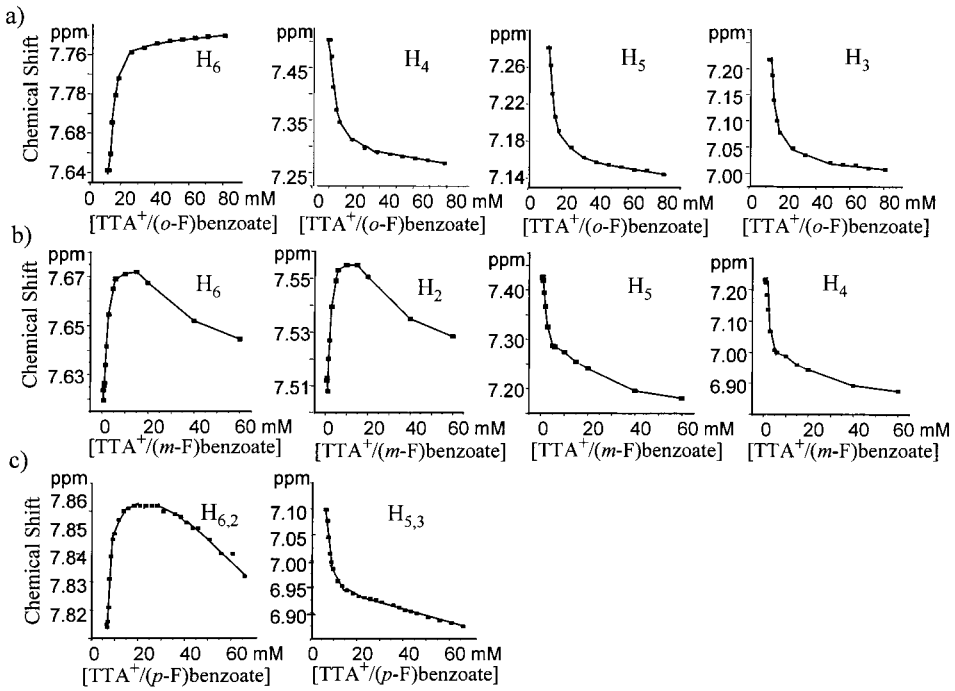

Figure 6. Expanded regions of the graphs in which the chemical shifts of the benzoate protons are plotted versus increasing TTA^+/fluorobenzoate concentrations for (a) TTA^+/*ortho*-fluorobenzoate, (b) TTA^+/*meta*-fluorobenzoate, and (c) TTA^+/*para*-fluorobenzoate. In contrast to TTA^+/*ortho*-fluorobenzoate, the chemical shifts of the signals for H_6 and H_2 for TTA^+/*meta*- and *para*-fluorobenzoate reveal a remarkable behavior: In the concentration range from the cmc to 10 times the cmc, these signals shift downfield to change direction and move upfield at concentrations 10 times the cmc. The signals of the remaining benzoate protons continue to shift upfield over the entire concentration range studied.

Table 1. The cmc Values, Fractional Ionization Constants α, and Percent Counterion Binding of the TTA^+/Fluorobenzoates

	cmc values (mM)						
micellar aggregates	surface tension[a]	conductivity[b]	^{1}H NMR[b,c]	averaged cmc's	α values	% counterion binding	log *P* benzoic acids[d]
TTA^+/*ortho*-fluorobenzoate	2.30	2.80	2.42	2.51	0.16	84	1.77
TTA^+/*meta*-fluorobenzoate	1.26	1.32	1.28	1.29	0.15	85	2.15
TTA^+/*para*-fluorobenzoate	1.30	1.42	1.43	1.38	0.16	84	2.08
TTA^+/*ortho*-toluate	2.35	2.50	nd	na	0.16	84	2.18
TTA^+/*meta*-toluate	1.08	1.08	nd	na	0.13	87	2.37
TTA^+/*para*-toluate	1.05	1.05	nd	na	0.12	88	2.27

[a] Data recorded at 295 K. [b] Data recorded at 298 K. [c] Determined from the average chemical shift values of selected surfactant and fluorobenzoate proton resonances. [d] Hydrophobicity values taken from Leo (ref 61). nd = not determined. na = not applicable.

cmc values were also deduced from the ^{13}C and ^{19}F NMR chemical shifts (Tables 3 and 4, respectively) and are comparable to those obtained by ^{1}H NMR spectroscopy. However, their margins of error are larger due to the lower intensity of the ^{13}C signals and the broadness of the ^{19}F resonance lines and are, therefore, not listed.

The cmc values determined by the three different methods (Table 1) are in good agreement with each other and are within the error limits of each of the experiments. Considering that the cmc's are not true critical points[45] and that different methods yield somewhat different values,[36] the small differences observed are not surprising. Among the three systems, TTA^+/*meta*- and *para*-fluorobenzoate have the greatest tendency to aggregate as is indicated by their low cmc values (1.29 and 1.38 mM, respectively), which are by a factor of 0.6 smaller than the cmc of the TTA^+/*ortho*-fluorobenzoate aggregates (2.51 mM). The difference in the cmc values is quite remarkable considering that all three surfactant systems have comparable high degrees of counterion binding as is reflected in the α values (Table 1). It shows that the cmc and the α values are not necessarily interrelated and that comparable degrees of counterion binding do not necessarily imply identical or similar cmc values. This statement diverges from investigations that have reported correlations between counterion binding and micelle formation.[19,54] However, as we[55] and others[29a,b,36] have shown convincingly, such relationships can be established when a few selected anions are studied but not when a larger number of counterions is investigated.

Growth to Rodlike Micelles. Growth from spherical to rodlike micelles is exhibited solely by TTA^+/*meta*- and *para*-fluorobenzoates. Its onset is clearly observable in the conductivity and the ^{1}H NMR plots of these aggregates (Figures 1b,c, 3, 4, 5b,c, and 6b,c), which reveal a second breakpoint at concentrations 10 times the cmc. This break, which is hereafter denoted the second cmc,[40,52,56] serves as indicator for the transformation from spherical to

(54) Selpúlveda, L.; Cortés, J. *J. Phys. Chem.* **1985**, *89*, 5322−5324.
(55) Bachofer, S. J.; Simonis, U.; Stiles, P. L. 219th National Meeting of the American Chemical Society, March 2000, Book of Abstracts, No. 268.
(56) Alargova, R. G.; Danov, K. D.; Petkov, J. T.; Kralchevsky, P. A.; Broze, G.; Mehreteab, A. *Langmuir* **1997**, *13*, 5544−5551.

rodlike micelles. Its use as a sphere-to-rod transition marker is not new to our studies. For mixed cationic micelles, Treiner et al.[52] related the second cmc to structural micelle changes, whereas Alargova et al.[56] interpreted the second change in the surface tension plot of anionic micelles as the sphere-to-rod transition. Applying a linear regression analysis to the conductivity data (Figure 1), the intersections of the two straight lines, where the onset of growth is proposed, are at 14 and 19 mM for TTA^+/*meta*- and *para*-fluorobenzoates, respectively. The corresponding values deduced from the ^1H NMR inverse plots are slightly larger, 15 mM for TTA^+/*meta*-fluorobenzoate and 22.5 mM for TTA^+/*para*-fluorobenzoates. A sample plot of the second cmc determination is included in Figure S3 (Supporting Information). Based on the observation that all three surfactants have nearly identical α values but that only *meta*- and *para*-fluorobenzoates induce growth, we suggest that the degree of counterion binding is a minor contributor to rod formation. As is discussed below, the positioning of the fluoro substituent at the benzene ring periphery combined with the intrinsic ability of the anion to form tight ion pairs and to reduce headgroup repulsions seem to be the main determinants of micelle growth. Underwood and Anacker[36] drew similar conclusions and showed for alkylammonium/benzoates that the mitigation of headgroup repulsion by the counterion is of greater importance for micelle formation than the degree of counterion binding. The groups of Magid,[35] Engberts,[29] and Kim[33] pointed out the importance of the loci of the anion in inducing micelle morphology changes by weakening the electrostatic repulsions. The laboratory of Romsted[42b] suggested recently that rod formation may require a significant fraction of headgroups and counterions to form hydrated tight ion pairs.

The ^1H NMR spectra reveal an additional marker for the onset of micelle growth. A remarkable chemical shift behavior is exhibited by the four aromatic protons of TTA^+/*meta*- and *para*-fluorobenzoates. At concentrations above the second cmc, the signals of the benzoate protons, which are described below to interact more strongly with the headgroups (H_2 and H_6), change direction and shift in the opposite way with an increase in TTA^+/fluorobenzoate concentration (Figures 5b,c and 6b,c). The resonances of the protons that are directed toward the palisade layer[5,57] (H_4 and H_5 of TTA^+/*meta*-fluorobenzoate; H_3 and H_5 of TTA^+/*para*-fluorobenzoate) continue to move in the same direction. In contrast, no reversal in chemical shift direction is observed for any of the *ortho*-fluorobenzoate resonances over the entire concentration range studied (Figures 5a and 6a). All four protons continue to shift in the same direction; H_3, H_4, and H_5 move upfield and H_6 shifts downfield. Thus, the reversal in chemical shift direction of the benzoate protons serves as a direct marker of the sphere-to-rod transition and micelle growth and illustrates that ^1H NMR spectroscopy provides a powerful tool to detect environmental changes accompanying micelle formation and growth. Before continuing our discussion, it should be noted that when referring to micellar structure the terminology detailed by Hiemenz and Rajagopalan[5] was adopted. Although not always well defined in thickness, the terms Stern and palisade layer are employed throughout the text for reasons of brevity, clarity, and simplicity. Acknowledging that micelles exist in a state of dynamic equilibrium, the term regions is nevertheless used when referring to micelle areas. The region that consists of surfactant heads and bound counterions is termed the Stern layer, and the hydrated shell between the inner central core and the polar heads is termed the palisade layer.

Orientation and Location of the Fluorobenzoates at the TTA^+−Micellar Interface: Trends Observed in the NMR Spectra. The findings above that the formation of tight ion pairs and the concomitant mitigation of headgroup repulsions by the counterion, which enable increased surfactant packing, are the major contributors to micelle growth is supported by the orientation and location of the fluorobenzoates at the micellar interface. These were deduced from the concentration dependence, magnitude, and direction of the ^1H, ^{13}C, and ^{19}F chemical shifts of the benzoate and/or the surfactant resonances. The ^1H and ^{19}F NMR spectra of the TTA^+/fluorobenzoates were compared to those of the fluorobenzoate ion alone dissolved in D_2O, in ND_3/ND_4^+ buffered D_2O at pH = 10, and in CD_3OD and $CDCl_3$ with added triethylamine. For the discussion below, it is important to note that every time a reference is made to the fluorobenzoates in methanol or chloroform the addition of equimolar amounts of the amine is implied. The amine was added to CD_3OD and $CDCl_3$ to establish that the chemical shifts of the fluorobenzoate nuclei in the micellar solutions are greatly affected by the polarity of the environment in which they reside. To this end, it was essential to ensure that the fluorobenzoate anions and not the benzoic acids were present in solution, which was guaranteed for the micellar solutions by the preparative ion exchange approach employed. Furthermore, differences in solvation of the benzoates also contribute to the NMR resonance patterns, which accounts for chemical shift variations among the anions incorporated into the micellar environments and dissolved in the pure solvents.

Trends Observed in the NMR Spectra of TTA^+/*ortho*-Fluorobenzoate: ^1H Chemical Shifts of the Benzoate Resonances. The ^1H NMR spectra of TTA^+/*ortho*-fluorobenzoate show four signals for the benzoate protons, an apparent triplet comprised of doublets of doublets for the most downfield-shifted proton H_6, a multiplet for H_4, and triplets for H_5 and H_3 (Figure 2). Below the cmc (0.94 to 1.88 mM), these protons remain in the same chemical environment as is evidenced by the negligible chemical shift changes (Table 2). In this region, the resonance positions are determined by the presence of predominately TTA^+/*ortho*-fluorobenzoate monomers, most likely in equilibrium with premicellar aggregates, which assemble at the cmc to form spherical micelles. At surfactant concentrations just above the cmc, the chemical environments of the benzoate protons change abruptly. Proton H_6 becomes deshielded and moves downfield (Figure 2). Above 25 mM TTA^+/*ortho*-fluorobenzoate concentrations, the chemical shift of H_6 remains essentially unchanged to reach a value of 7.779 ppm at 70 mM, which corresponds to the resonance position of the *ortho*-fluorobenzoate anion, when it is dissolved in a solvent that is less polar than water and methanol, but more polar than chloroform (δ of *ortho*-fluorobenzoate: H_6 = 7.559 ppm in D_2O, 7.670 ppm in CD_3OD, and 7.867 ppm in $CDCl_3$). In contrast to H_6, the remaining protons H_3, H_4, and H_5 experience upfield shifts in the surfactant concentration range from the cmc to about 25 mM and change insignificantly above this concentration with the largest shifts of 0.022 ppm being observed for H_3 and H_4. At 70 mM, the chemical shifts of H_3, H_4, and H_5 [(δ (ppm) = 7.008, 7.268, and 7.134, respectively] approach those of *ortho*-fluorobenzoate, when it is dissolved in chloroform (δ of *ortho*-fluorobenzoate in $CDCl_3$: H_3 = 7.038 ppm, H_4 = 7.321 ppm, and H_5 = 7.106 ppm; as compared to δ of

(57) Rosen, M. J. In *Surfactants and Interfacial Phenomena*, 2nd ed.; Wiley-Interscience: New York, 1989; pp 173−174.

Table 2. TTA^+/Fluorobenzoate ^1H Chemical Shifts at 298 K with Increasing Surfactant Concentration

(a) TTA^+/*ortho*-Fluorobenzoate

	δ [ppm]									
$[TTA^+/X^-]$ [mM]	H_3	H_4	H_5	H_6	$^+N(CH_3)_3$	α-CH_2	β-CH_2−	γ-CH_2−	$(-CH_2-)_n$	ω-CH_3
0.94	7.218	7.504	7.271	7.643	3.141	3.343	1.822	1.397	1.324	0.905
1.88	7.217	7.503	7.271	7.643	3.140	3.342	1.821	1.397	1.324	0.905
2.81	7.187	7.472	7.252	7.659	3.127	3.305	1.767	merged	1.333	0.923
3.75	7.140	7.413	7.221	7.691	3.107	3.246	1.688	1.269	1.358	0.954
5.62	7.101	7.369	7.196	7.719	3.090	3.196	1.619	1.209	1.383	0.981
7.50	7.078	7.346	7.181	7.736	3.081	3.170	1.582	1.173	1.394	0.994
15.0	7.049	7.313	7.163	7.763	3.070	3.135	1.535	1.122	1.411	1.014
22.5	7.035	7.297	7.152	7.767	3.064	3.124	1.503	1.102	1.413	1.018
30.0	7.028	7.290	7.147	7.772	3.063	3.117	merged	1.093	1.416	1.021
37.5	7.021	7.285	7.144	7.774	3.063	3.113	merged	1.088	1.417	1.024
45.0	7.017	7.280	7.142	7.776	3.061	merged	merged	1.085	1.418	1.026
52.5	7.016	7.278	7.139	7.777	3.060	merged	merged	1.079	1.419	1.027
60.0	7.010	7.274	7.138	7.779	3.061	merged	merged	merged	1.419	1.029
70.0	7.008	7.268	7.134	7.779	3.058	merged	merged	merged	1.422	1.029

(b) TTA^+/*meta*-Fluorobenzoate

	δ [ppm]									
$[TTA^+/X^-]$ [mM]	H_2	H_4	H_5	H_6	$^+N(CH_3)_3$	α-CH_2	β-CH_2−	γ-CH_2−	$(-CH_2-)_n$	ω-CH_3
0.60	7.512	7.232	7.425	7.624	3.057	3.260	1.736	1.319	1.240	0.821
0.80	7.513	7.234	7.427	7.620	3.059	3.260	1.732	1.308	1.242	0.814
1.00	7.512	7.224	7.420	7.626	3.052	3.247	1.725	1.296	1.241	0.811
1.20	7.508	7.222	7.419	7.627	3.051	3.244	1.710	1.289	1.242	0.810
1.50	7.520	7.182	7.395	7.634	3.031	3.191	1.644	1.226	1.257	0.835
2.00	7.527	7.136	7.367	7.642	3.009	3.131	1.565	1.167	1.280	0.875
3.00	7.540	7.067	7.325	7.655	2.976	3.035	1.453	1.062	1.315	0.914
5.00	7.549	7.007	7.288	7.665	2.947	merged	merged	merged	1.341	0.944
6.00	7.553	7.000	7.285	7.669	2.950	merged	merged	merged	1.340	0.943
10.0	7.555	6.987	7.275	7.671	2.939	merged	merged	merged	1.351	0.956
15.0	7.555	6.959	7.254	7.672	2.930	merged	merged	merged	1.354	0.963
20.0	7.551	6.944	7.241	7.668	2.927	merged	merged	merged	1.355	0.963
40.0	7.535	6.893	7.195	7.652	2.915	merged	merged	merged	1.352	0.962
60.0	7.529	6.874	7.180	7.645	2.911	merged	merged	merged	1.349	0.960

(c) TTA^+/*para*-Fluorobenzoate

	δ [ppm]							
$[TTA^+/X^-]$ [mM]	$H_{2,6}$	$H_{3,5}$	$^+N(CH_3)_3$	α-CH_2	β-CH_2−	γ-CH_2−	$(-CH_2-)_n$	ω-CH_3
0.80	7.815	7.099	3.023	3.226	1.707	1.284	1.205	0.786
1.20	7.816	7.098	3.023	3.224	1.702	1.283	1.206	0.787
1.60	7.821	7.077	3.002	3.173	1.630	merged	1.216	0.806
2.00	7.831	7.045	2.974	3.100	1.513	merged	1.241	0.833
2.66	7.839	7.014	2.945	3.026	1.451	merged	1.266	0.861
3.33	7.845	6.997	2.930	2.986	1.405	merged	1.282	0.877
8.00	7.855	6.951	2.890	merged	merged	merged	1.318	0.915
12.5	7.857	6.937	2.879	merged	merged	merged	1.328	0.925
15.0	7.857	6.931	2.874	merged	merged	merged	1.331	0.928
20.0	7.857	6.926	2.870	merged	merged	merged	1.333	0.931
30.0	7.854	6.914	2.865	merged	merged	merged	1.335	0.933
40.0	7.849	6.899	2.861	merged	merged	merged	1.333	0.932
50.0	7.840	6.885	2.856	merged	merged	merged	1.330	0.928
60.0	7.832	6.874	2.851	merged	merged	merged	1.327	0.924

ortho-fluorobenzoate in CD_3OD: $H_3 = 7.077$ ppm, $H_4 = 7.369$ ppm, and $H_5 = 7.180$ ppm). The insignificant chemical shift changes above 25 mM reveal that all protons remain in essentially the same environments, which implies that the micelles do not undergo structural changes and remain spherical even at 70 mM TTA^+/fluorobenzoate concentrations. In accordance, no second cmc is observable in either the conductivity or the NMR plots (Figures 1a, 5a, and 6a, respectively).

In agreement with conclusions drawn in the chloro- and hydroxybenzoate studies of Kreke et al.[20] and Manohar et al.,[9,25] their upfield shifts indicate that H_3, H_4, and H_5 move upon micelle formation from a polar aqueous into a relatively nonpolar hydrocarbon-like environment, whereas H_6 remains exposed to a more polar medium as is revealed by its downfield-shifted signal. These shifts and their directions are closely paralleled by those of *ortho*-chlorobenzoates in cationic micelles[17−20] and suggest that the *ortho*-fluorobenzoate ions adopt preferential orientations at the micellar interface binding with a tilted orientation. This tilt places only the carboxylate group close to the headgroup region of the micelle, whereas the benzene ring moves toward the palisade layer of the micelle. This average location may be unexpected but can be easily rationalized when one considers the structure of the anion and the environments in which the benzoate protons and the fluoro and carboxylate substituents prefer to reside. The hydrophilic carboxylate group favors on average a more polar environment and, therefore, orients in the Stern layer. This positioning causes H_6 to move toward the $^+N(CH_3)_3$ headgroups in the Stern layer, which explains its downfield shift. The remaining protons and the fluorine atom prefer average positions in less polar environments, as is expressed in their upfield shifts, which

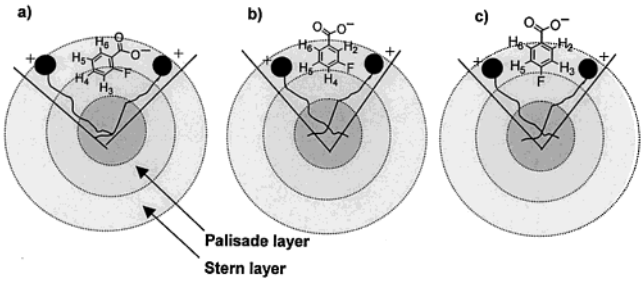

Figure 7. Cartoons of the proposed average orientation and location of (a) *ortho*-fluorobenzoate, (b) *meta*-fluorobenzoate, and (c) *para*-fluorobenzoate in TTA^+ micelles.

suggests their movement toward the palisade layer. A cartoon of the anion's orientational binding at the TTA^+ micelle is given in Figure 7a. The chemical shift changes observed for the aromatic ring protons support this orientational binding and indicate that the anion is on average surrounded by a nonpolar micellar environment. Based on the chemical shift trends observed, the potential for tangential binding of the anion at the interface is not very likely, since for such a binding the proton resonances would mirror those of the fluorobenzoates solvated in aqueous environments only.

^{19}F and ^{13}C Chemical Shifts of the Benzoate Resonances. Additional support that the aromatic ring of the *ortho*-fluorobenzoate is directed toward the palisade layer of TTA^+ micelles is provided by the ^{19}F and ^{13}C chemical shift trends. Below the cmc, the fluorine nucleus gives rise to the signal at −116.55 ppm, when referenced to CCl_3F, which is split by a three-bond coupling to H_3 and by long-range couplings to H_4 and H_6. With increasing concentration, the resonance broadens and moves downfield to −114.12 ppm at 70 mM, which matches the ^{19}F peak position of the *ortho*-fluorobenzoate alone, when it is dissolved in chloroform (δ = −114.1 ppm). This resonance is observed in CD_3OD at −115.7 ppm and in the buffered D_2O solution at −116.7 ppm. This comparison reveals that the fluorine nucleus localizes in a micellar environment with a polarity approaching that of $CDCl_3$, a relatively nonpolar environment. However, its shift in the downfield direction upon micelle formation suggests that the ^{19}F nucleus is not buried in the micellar core but remains oriented toward the palisade layer. The ^{13}C chemical shift trends, which parallel those of their attached protons, support this conclusion and are best explained by the environments into which the carbon nuclei are drawn upon micelle formation. With increasing TTA^+/*ortho*-fluorobenzoate concentration, the signals of C_2, C_3, C_4, and COO^- move upfield (Table 3), and C_6 shifts downfield, whereas the peak positions of C_1 and C_5 remain essentially unchanged. The largest changes are observed for the ^{13}C resonance of the COO^- group followed by the signals of C_6 and C_4. Their upfield shifts indicate that C_2, C_3, and C_4 are surrounded by the shielding environment of the micellar hydrocarbon surfactant chains and that the COO^- group is drawn from the polar aqueous monomer surfactant environment into that of the highly charged interface of the Stern layer. Upon micellization, C_6 becomes deshielded, which suggests that micelle formation exposes this carbon to the same interface. The insignificant shifts of C_1 and C_5 indicate that the water boundary in the TTA^+/*ortho*-fluorobenzoate micelles exists between these carbons, which supports the tilted orientation of the *ortho*-fluorobenzoates at the micellar interface. The comparison of the ^{13}C chemical shifts of C_2, C_3, C_4, C_6, and COO^- in TTA^+ micelles (Table 3a) to those of the anion alone dissolved in solvents of differing polarity emphasizes that in the micellar solution the ^{13}C chemical shifts approach the values of the *ortho*-fluorobenzoate ion dissolved in chloroform. This confirms that parts of the aromatic rings of the *ortho*-fluorobenzoate ions are directed toward the palisade layer with only C_6 and the carboxylate group being proximate to the headgroup region of the Stern layer.

^{1}H and ^{13}C Chemical Shift of the Surfactant Resonances. The proton and carbon resonance shifts of the surfactants (Figure 2) are in agreement with the proposed orientational binding of the *ortho*-fluorobenzoates at the micellar interface and provide additional evidence for the spherical shapes of TTA^+/*ortho*-fluorobenzoate micelles. Above the cmc, the ^{1}H resonances of the headgroup region [$^+N(CH_3)_3$ and α, β, γ, δ-CH_2] move upfield. The α, β, γ, δ-CH_2 protons are most shifted by the magnetic anisotropy of the benzoate ring[20,30,50] with the largest changes of 0.34 and 0.32 ppm being observed for the β and γ, δ-CH_2 resonances. The $^+N(CH_3)_3$ resonance shifts by only 0.069 ppm from 3.127 ppm at 2.81 mM to 3.058 ppm at 70.0 mM. This shift is notable but by a factor of 5 smaller than that of the β and γ, δ-CH_2 protons, which suggests that the aromatic rings of the *ortho*-fluorobenzoate ions interact only weakly with the charged $^+N(CH_3)_3$ headgroups. This is corroborated by the comparison of the ^{1}H resonance positions of TTA^+/*ortho*-fluorobenzoate and TTAB micelles. The $^+N(CH_3)_3$ protons of 50 mM TTAB resonate at 3.123 ppm, whereas the corresponding signal of 50 mM TTA^+ comicellized with *ortho*-fluorobenzoates is observed at 3.060 ppm. The difference is small (0.063 ppm) and indicates that the $^+N(CH_3)_3$ protons are the least shifted by the magnetic anisotropy of the aromatic ion, which corroborates that the *ortho*-fluorobenzoates are not intercalated among the headgroups.

In contrast to the ^{1}H signals of the headgroup region, the remaining alkyl chain protons (the bulk of the methylene and the ω-CH_3 protons) are deshielded by the aromatic ring current and shift downfield. Noteworthy is the large shift of the ω-CH_3 group, which moves downfield from 0.923 ppm at 2.81 mM to 1.027 ppm at 50.0 mM. When compared to TTAB alone at 50 mM, this shift is even more pronounced. The chemical shift difference of the ω-CH_3 group in the micellar solution and in TTAB amounts to 0.202 ppm clearly demonstrating the effects of the aromatic ring current on these surfactant resonances of TTA^+/*ortho*-fluorobenzoate micelles. The large shift of methylene and the ω-CH_3 protons provides an additional argument against the tangential binding of the *ortho*-fluorobenzoates at the micellar interface. Above 30 mM, all TTA^+ resonances shift insignificantly (0.01−0.02 ppm), a behavior that is paralleled by TTAB micelles, which stay spherical even at very high surfactant concentrations.[49,52] Therefore, it can be concluded that TTA^+/*ortho*-fluorobenzoate micelles do not grow and stay spherical over the large concentration range studied,[49,52] as is also indicated by the ^{13}C chemical shifts of the surfactant chain carbon resonances (Table 3a), which are less pronounced than those in the ^{1}H or ^{19}F spectra. Upon micelle formation, all ^{13}C resonances with the exception of C_1 shift downfield with the largest chemical shift changes observed for C_4 followed by C_{13}, C_{12}, and C_3. Above 30 mM concentrations, the carbon resonances remain essentially unchanged.

Trends Observed in the NMR Spectra of TTA^+/*meta* and *para*-Fluorobenzoate. Both the TTA^+/*meta*- and *para*-fluorobenzoate systems exhibit similar chemical shift behaviors, which are distinctively different from those of the TTA^+/*ortho*-fluorobenzoate aggregates.

^{1}H Chemical Shifts of the Fluorobenzoate Resonances. Below the cmc, the NMR spectra of both TTA^+/*meta*- and

Table 3. TTA^+/Fluorobenzoate ^{13}C Chemical Shifts with Increasing Concentration at 298 K

(a) TTA^+/*ortho*-Fluorobenzoate, δ [ppm]

$[TTA^+/X^-]$	*ortho*-fluorobenzoate resonances							TTA^+ resonances							
[mM]	C_1	C_3	C_4	C_5	C_6	C−F	COO^-	$^+N(CH_3)_3$	C_1	C_2	C_3	C_4	C_{12}	C_{13}	C_{14}
2.81		118.58	134.05	126.56	132.58			55.28	69.26	24.79	28.00	30.80	24.71	33.90	16.04
3.75		118.51	133.79	126.47	132.94			55.27	69.11	24.90	28.17	31.07	24.90	34.14	16.18
5.62	129.15	118.45	133.56	126.38	133.24	162.72	174.45	55.29	68.99	24.99	28.30	31.30	25.07	34.35	16.30
7.50		118.43	133.49	126.35	133.43			55.28	68.95	25.03	28.36	31.42	25.15	34.46	16.36
15.0		118.41	133.40	126.29	133.69			55.29	68.86	25.10	28.46	31.58	25.26	34.60	16.43
22.5		118.39	133.38	126.27	133.78			55.29	68.83	25.11	28.49	31.63	25.30	34.65	16.45
30.0	129.15	118.39	133.36	126.26	133.83	163.07		55.30	68.82	25.13	28.50	31.65	25.31	34.67	16.46
37.5		118.38	133.34	126.25	133.85	163.09	173.15	55.29	68.80	25.13	28.51	31.67	25.32	34.68	16.47
45.0	129.14	118.38	133.33	126.24	133.89	163.11	173.09	55.30	68.80	25.14	28.52	31.68	25.33	34.69	16.47
52.5	129.17	118.37	133.31	126.24	133.89	163.10	173.08	55.29	68.80	25.13	28.52	31.68	25.33	34.70	16.47
60.0	129.14	118.38	133.31	126.23	133.91	163.12	173.02	55.30	68.78	25.14	28.52	31.69	25.34	34.70	16.47
70.0	129.13	118.38	133.31	126.23	133.94	163.13	172.99	55.30	68.79	25.14	28.53	31.70	25.34	34.71	16.47

(b) TTA^+/*meta*-Fluorobenzoate, δ [ppm]

$[TTA^+/X^-]$	*meta*-fluorobenzoate resonances							TTA^+ resonances							
[mM]	C_1	C_3	C_4	C_5	C_6	C−F	COO^-	$^+N(CH_3)_3$	C_1	C_2	C_3	C_4	C_{12}	C_{13}	C_{14}
5.0		118.29		132.07	127.46		174.51	55.23	68.91	25.12	28.49	31.59	25.24	34.56	16.40
6.0	142.54	118.30	119.58	132.06	127.51	164.91		55.25	68.91	25.13	28.51	31.61	25.25	34.58	16.40
10.0	142.57	118.34	119.62	132.05	127.55	164.91	174.28	55.25	68.89	25.15	28.53	31.66	25.29	34.64	16.42
15.0	142.41	118.39	119.58	131.99	127.60	164.89	173.88	55.25	68.84	25.17	28.57	31.73	25.32	34.68	16.44
20.0	142.54	118.38	119.49	131.97	127.59	164.89	173.87	55.27	68.84	25.19	28.59	31.76	25.33	34.69	16.46
40.0	142.52	118.42	119.55	131.88	127.60	164.87	173.38	55.24	68.75	25.20	28.60	31.78	25.33	34.68	16.44
60.0	142.48	118.42	merged	131.88	127.60	164.88	173.31	55.25	68.69	merged		merged	25.33	34.69	16.44

para-fluorobenzoate show little if any change in the chemical shifts of the aromatic protons as the surfactant concentration is increased (Table 2b,c; Figures 3, 4, 5b,c, and 6b,c). In the concentration range from the cmc to the second cmc, pronounced chemical shift changes are observed although no visual increase in solution viscosity is noticeable. For TTA^+/*meta*-fluorobenzoate, the resonances of H_2 and H_6 shift downfield by 0.043 and 0.045 ppm, respectively, in the concentration range of 1.0 mM, which is just below the cmc, to 15 mM, whereas those of protons H_4 and H_5 move upfield and give rise to larger chemical shift changes of 0.237 ppm for H_4 and 0.145 ppm for H_5 (Table 2b). For TTA^+/*para*-fluorobenzoate micelles, the resonance of the chemically equivalent protons H_2 and H_6 shifts downfield by 0.041 ppm in the concentration range from 1.20 (at the cmc) to 22.5 mM, whereas the signal of the chemically equivalent protons H_3 and H_5 moves upfield by 0.171 ppm. At the second cmc (15 and 22.5 mM for TTA^+/*meta*-and *para*-fluorobenzoates, respectively) the benzoate protons display a remarkable behavior (Figures 5b,c and 6b,c). For both micellar systems, the signals of H_2 and H_6 change direction and start moving upfield instead of downfield. The resonances of H_4 and H_5 for TTA^+/*meta*-fluorobenzoate and H_3 and H_5 for TTA^+/*para*-fluorobenzoate continue to shift upfield; however, the observed chemical shift changes are less pronounced (Table 2). At concentrations above the second cmc, all protons continue to move, but the shifts are small [$\Delta\delta$ (TTA^+/*meta*-fluorobenzoate): 0.03 ppm for H_2/H_6 and 0.08 ppm for H_4/H_5; $\Delta\delta$ (TTA^+/*para*-fluorobenzoate): 0.03 ppm for H_2/H_6 and 0.05 ppm for H_3/H_5).

The chemical shift trends, which are similar to those reported for chlorobenzoates in CTA^+ [18−20] or in $C_{22}N(CH_3)_3^+$ micelles,[17] are best explained by the location and orientation of the *meta*- and *para*-fluorobenzoates at the interface, which is schematically drawn in the cartoons in Figure 7b,c, and by micelle growth. In the surfactant range from the cmc to the second cmc, spherical micelles are the predominate species in solution. Micelle formation leads to the shielding of H_4 and H_5 for TTA^+/*meta*-fluorobenzoate and H_3 and H_5 for TTA^+/*para*-fluorobenzoate, which implies that these protons are oriented toward the palisade layer and are shifted upfield by the surrounding hydrocarbon chains. In contrast, H_2 and H_6 become deshielded upon micellization, which suggests that these protons are exposed to the aqueous environment of the water/micelle interface. When the chemical shifts of the fluorobenzoate protons in TTA^+ micelles are compared to those of the anion alone dissolved in buffered D_2O, CD_3OD, or $CDCl_3$, it is evident that H_2 and H_6 remain on average in an environment which approaches the polarity of D_2O (δ *meta*-fluorobenzoate (20.0 mM): H_2 = 7.736 ppm in $CDCl_3$, 7.628 ppm in CD_3OD, and 7.505 ppm in buffered D_2O and H_6 = 7.845 ppm in $CDCl_3$, 7.762 ppm in CD_3OD, and 7.628 ppm in buffered D_2O; as compared to δ TTA^+/*meta*-fluorobenzoate: H_2 = 7.551 ppm and H_6 = 7.668 ppm. δ TTA^+/*para*-fluorobenzoate: $H_{2,6}$ = 8.082 ppm in $CDCl_3$, 8.049 ppm in CD_3OD, and 7.844 ppm in buffered D_2O; as compared to δ TTA^+/*meta*-fluorobenzoate: $H_{2,6}$ = 7.857 ppm.). For H_4 and H_5 of TTA^+/*meta*-fluorobenzoate or H_3 and H_5 of TTA^+/*para*-fluorobenzoate, the comparison is not as convincing as for H_2 and H_6 due to the larger chemical shift deviations observed between the micellar solutions and the pure solvents, which is most likely attributable to solvation effects. Nevertheless, the trends observed indicate that H_4 and H_5 of TTA^+/*meta*-fluorobenzoate or H_3 and H_5 of TTA^+/*para*-fluorobenzoate are immersed in a micellar medium, which is closer in polarity to $CDCl_3$ than to methanol or water. This suggests that micelle formation draws the fluorine nuclei more deeply into the Stern layer (δ *meta*-fluorobenzoate (20.0 mM): H_4 = 7.094 ppm in $CDCl_3$, 7.137 ppm in CD_3OD, and 7.256 ppm in buffered D_2O and H_5 = 7.326 ppm in $CDCl_3$, 7.368 ppm in CD_3OD, and 7.434 ppm in buffered D_2O; as compared to δ TTA^+/*meta*-fluorobenzoate: H_4 = 6.944 ppm and H_5 = 7.241 ppm. δ *para*-fluorobenzoate: $H_{3,5}$ = 7.065 ppm in $CDCl_3$, 7.095 ppm in CD_3OD, and 7.162 ppm in buffered D_2O; as compared to δ TTA^+/*para*-fluorobenzoate: $H_{3,5}$ = 6.926 ppm.). The reversal in chemical shift direction of the protons at the water/micelle interface (H_2 and H_6) at the second cmc is explainable only by morphology changes from initially spherical to rodlike micelles, which is also supported by slope changes in the conductivity plots.[52] As sensed by the chemical shifts,

Table 4. TTA^+/Fluorobenzoate ^{19}F Chemical Shifts with Increasing Concentration at 298 K

TTA^+/*ortho*-fluorobenzoate		TTA^+/*meta*-fluorobenzoate		TTA^+/*para*-fluorobenzoate	
[mM]	δ [ppm]	[mM]	δ [ppm]	[mM]	δ [ppm]
0.94	−116.56	0.6	−114.39	0.8	−110.88
1.88	−116.55	1.0	−114.24	1.2	−110.88
2.81	−116.21	1.2	−114.36	1.6	−110.85
3.75	−115.78	1.5	−114.27	2.0	−110.81
5.62	−115.30	2.0	−114.19	2.7	−110.76
7.50	−115.03	3.0	−114.08	4.0	−110.72
15.0	−114.59	5.0	−113.94	6.0	−110.70
22.5	−114.43	6.0	−113.94	10.0	−110.65
30.0	−114.35	10.0	−113.89	15.0	−110.63
37.5	−114.29	15.0	−113.79	20.0	−110.63
45.0	−114.28	20.0	−113.80	30.0	−110.63
52.5	−114.27	40.0	−113.71	40.0	−110.63
60.0	−114.23	60.0	−113.70	50.0	−110.63
70.0	−114.12			60.0	−110.64

rod formation moves the protons away from the water/micelle interface and positions them deeper in the Stern layer in closer proximity to the less polar environment of the palisade layer, which explains the upfield shifts of H_2 and H_6. Protons H_4/H_5 for TTA^+/*meta*-fluorobenzoate and H_3/H_5 for TTA^+/*para*-fluorobenzoate continue to interact more strongly with the surfactant chains, which accounts for their continued upfield shifts. Thus, the ^1H NMR data provide evidence for the following: (i) Growth occurs in two stages as was recently demonstrated by cryo-TEM studies of Bernheim-Groswasser et al.,[58] which revealed that above the cmc all micelles are small and globular. Above the second cmc, these aggregates coexist with much longer micelles. (ii) The transformation from spherical to rodlike micelles is a gradual rather than an abrupt process as is revealed by the pronounced chemical shift changes of the *meta*- and *para*-fluorobenzoate protons. This finding emphasizes the idea brought forward by Magid et al. of a region of growth.[19,35] In contrast to the abrupt, sharp change at the cmc, the transition to rodlike micelles at the second cmc is smooth and continuous, which is also proposed by the theoretical model developed by May and Ben-Shaul.[40b]

^{19}F Chemical Shifts of the Benzoate Resonances. The chemical shift changes observed for the ^{19}F nuclei of TTA^+/*meta*- and *para*-fluorobenzoates are very small in comparison to those of the *ortho*-fluorobenzoate micelles and are, therefore, of lesser diagnostic value. For TTA^+/*meta*-fluorobenzoates, the ^{19}F nucleus of the 0.6 mM solution resonates at −114.4 ppm relative to $CFCl_3$ (Table 4) and upon micelle formation moves downfield to reach a value of −113.7 ppm at 60 mM. For TTA^+/*para*-fluorobenzoates, the ^{19}F signal shifts from −110.9 ppm at 0.8 mM surfactant concentration to −110.6 ppm at 60 mM (Table 4). The small shift changes indicate that the chemical environments of the ^{19}F nuclei for both TTA^+/*meta*- and *para*-fluorobenzoates do not change significantly upon micelle formation and growth, which suggests that the fluorobenzoates are solvated in the Stern layer with the fluoro substituents being drawn into a slightly lower polarity environment as is schematically shown in the cartoons in Figure 7b,c. This positioning is consistent with the downfield direction of the ^{19}F chemical shifts and the movement of the ^{19}F resonance positions toward a medium that is less polar than water or methanol but more polar than chloroform as is revealed by the ^{19}F chemical shift comparisons of the anions in TTA^+ micelles and in the pure solvents (δ *meta*-fluorobenzoate = −115.4 ppm in D_2O buffer, −114.2 ppm in CD_3OD, and −112.4 ppm in $CDCl_3$ as compared to −113.7 ppm for TTA^+/*meta*-fluorobenzoate; δ *para*-fluorobenzoate = −112.9 ppm in D_2O buffer, −111.8 ppm in CD_3OD, and −108.6 ppm in $CDCl_3$ as compared to −110.6 ppm for TTA^+/*para*-fluorobenzoate).

^{13}C Chemical Shifts of the Benzoate Ion Resonances. Carbon-13 spectra of selected TTA^+/*meta*-fluorobenzoate samples above the cmc were acquired at surfactant concentrations ranging from 6.0 to 60.0 mM to determine the average location of the fluorobenzoate anions at the micellar interface. With increasing TTA^+/*meta*-fluorobenzoate concentration, upfield shifts are observed for C_1 (0.06 ppm), C_3 (0.02 ppm), C_4 (0.43 ppm), C_5 (0.18 ppm), and the carbon of the COO^- group (1.21 ppm). The upfield shifts of C_3, C_4, and C_5, which parallel those of the corresponding protons, indicate that these carbons are embedded in the lower polarity environment of the Stern layer, when micelles are formed. The remaining resonances of C_2 and C_6 give rise to downfield shifts of similar magnitudes, which agrees with the conclusion drawn for their attached protons that micelle formation leaves these nuclei exposed to the water/micelle interface. The large upfield shift of the COO^- carbon together with its movement toward the resonance position of *meta*-fluorobenzoate, when it is dissolved in a solvent less polar than water and more polar than chloroform, demonstrates that upon micelle formation this nucleus is also drawn into the Stern layer. For some of the carbon nuclei, such as C_1, an unusual chemical shift behavior is observed at the second cmc. A study is currently under way in our laboratories to determine if this behavior is attributable to micelle growth.

^1H Chemical Shift of the Surfactant Resonances. The chemical shift data of the TTA^+/*meta*- and *para*-fluorobenzoate surfactant protons (Table 2) indicate both that *meta*- and *para*-fluorobenzoates interact more strongly with the micellar headgroups than TTA^+/*ortho*-fluorobenzoate and that the aggregates undergo a transformation from spherical to rodlike micelles. The strong fluorobenzoate−headgroup interactions are directly reflected in the chemical shift changes observed for the headgroup proton signal. When the concentration-dependent ^1H NMR spectra of all TTA^+/fluorobenzoates are compared, the most striking difference is the large chemical shift change observed for the headgroup resonance. At concentrations ranging from about 1.0 to 60.0 mM, the $^+N(CH_3)_3$ resonance of the *meta*-fluorobenzoate aggregates shifts upfield by 0.140 ppm and that of TTA^+/*para*-fluorobenzoates, by 0.172 ppm (Table 2). These shifts are significantly larger than those of the $^+N(CH_3)_3$ signal of TTA^+/*ortho*-fluorobenzoates, which moves only by 0.080 ppm in the comparable concentration range, and imply that *meta*- and *para*-fluorobenzoates interact more strongly with the micellar headgroups than *ortho*-fluorobenzoates. This is only possible when the carboxylate and the headgroup are in close proximity to each other, and the anions are intercalated among the $^+N(CH_3)_3$ headgroups, such that tight ion pairs are formed. This intercalation reduces the repulsive headgroup interactions, which allows the headgroups to pack more tightly and consequently to grow. The strong benzoate−headgroup interactions are even more pronounced when the chemical shifts of the TTA^+/*meta- and para*-fluorobenzoate aggregates are compared to those of TTAB micelles. As is exemplified for TTA^+/*para*-fluorobenzoates at 50 mM, the $^+N(CH_3)_3$ protons of this aggregate give rise to the peak at 2.856 ppm, whereas the corresponding TTAB signal is shifted downfield by 0.267 ppm to resonate at 3.123 ppm. The significantly

(58) Bernheim-Groswasser, A.; Zana, R.; Talmon, Y. *J. Phys. Chem. B* **2000**, *104* (51), 12192−12201.

smaller shift of the ω-CH_3 signal (0.103 ppm), which is observed at 0.928 ppm for the benzoate aggregate and at 0.825 ppm for TTAB micelles, agrees with the idea that *meta*- and *para*-fluorobenzoate strongly interact with the TTA^+ headgroups and not the micellar interior.

Factors Leading to Aggregate Growth. The chemical shift analyses discussed above indicate that the average orientation and location of the fluorobenzoates in TTA^+ micelles is an important factor in inducing growth. All anions adopt time-averaged positions at the micellar interface as is reflected in the polarity of the micellar environment, in which the anions reside. The chemical shift comparison of the fluorobenzoate resonances in micellar solution and in a buffered aqueous solution or in a relatively nonpolar solvent, such as chloroform, suggests that on average all three anions penetrate TTA^+ micelles, however, at differing depths. The *meta*- and *para*-fluorobenzoates localize in the Stern layer and are intercalated among the micellar $^+N(CH_3)_3$ headgroups. In contrast, the *ortho*-fluorobenzoates bind with a tilted orientation to the micellar interface and penetrate the Stern layer to move closer to the palisade layer. The tilted orientation together with the deeper penetration does not enable the *ortho*-fluorobenzoates to reduce the electrostatic headgroup repulsions, and consequently the micelles stay spherical.

The polarity of the environment in which the counterions reside provides a powerful argument not only to deduce the average location of the fluorobenzoates at the micellar interface but also to explain why certain micellar aggregates grow and change shape whereas others do not and remain spherical. The chemical shift data of TTA^+/*meta*- and *para*-fluorobenzoates demonstrate that aggregate growth is induced when the fluorobenzoates intercalate among the $^+N(CH_3)_3$ heads. This intercalation decreases unfavorable headgroup repulsions and allows for the formation of tight ion pairs and consequently for a more efficient packing of the surfactant chains, which leads to an increase in the aggregation number[35,39,51] and aggregate growth at total surfactant concentrations above the second cmc. In support of this conclusion are reports by Engberts et al.,[29] Lin et al.,[22] Lindemuth and Bertrand,[51] and Magid et al.,[19−21,35] which have established that cationic surfactants associate to rodlike micelles, if the headgroups are allowed to pack tightly. A surfactant with a high degree of counterion binding may overcome headgroup repulsion by holding the oppositely charged counterion between the headgroups, such that their repulsions are repressed and rod-shaped micelles become favored.[51] The importance of reducing headgroup repulsions is emphasized in studies of CTA^+ aggregates, which grow to form rodlike micelles in the presence of *meta*- and *para*-chlorobenzoates, but not in the presence of *ortho*-chlorobenzoate unless the solutions are subjected to high ionic strength.[35] Studies by Engberts et al. demonstrate that the intercalation of salicylate and *para*-chlorobenzoate among the headgroups allows the aggregate to grow,[29a,b] whereas benzoates, which do not bind among the headgroups, do not promote micelle growth, at least not at concentrations 20 times the cmc.

Two additional arguments, the depth of penetration[10,17−20] and the polarizability of the anion recently brought forward by Ducker et al.[59] and the group of Romsted,[42b] are self-consistent with the polarity argument and corroborate that the *ortho*-fluorobenzoate anions penetrate the TTA^+ interface more deeply than *meta*- and *para*-fluorobenzoates. To assess the depth of penetration, i.e., the proximity of the anions to the micellar surface, the differences in the magnitudes of the chemical shift values, the $\Delta\delta$ values, of the aromatic anion resonances are quite often used. On average, the $\Delta\delta$ values of the aromatic anion resonances, which are computed by subtracting the chemical shift value at 10 times the cmc from that at the cmc, are larger for the *ortho*-fluorobenzoate than for the *para*- and *meta*-fluorobenzoate aggregates, which confirms that *ortho*-fluorobenzoate penetrates the micellar interface more deeply than the other two anions. At first glance, the $\Delta\delta$ values of H_5 are puzzling, since they are somewhat larger for the *meta*- and *para*- than for *ortho*-fluorobenzoate micelles ($\Delta\delta$ = 0.17, 0.16, and 0.12 ppm for *meta*, *para*, and *ortho*-fluorobenzoate, respectively). However, the smaller chemical shift difference observed for H_5 of the *ortho*-fluorobenzoate anion can be rationalized, when the tilted orientation of this anion at the micellar interface is considered. The tilt moves H_5 closer to the water/micelle surface than in the case of *meta*- and *para*-fluorobenzoate micelles. The tilted orientation of the *ortho*-fluorobenzoates at the TTA^+ interface and their inherent deeper penetration are also manifested in the magnitudes of the chemical shift changes observed for H_3 ($\Delta\delta$ = 0.21 ppm) and H_4 ($\Delta\delta$ = 0.19 ppm), which are larger than those observed for H_5.

In terms of polarizability of the anion, Subramanian and Ducker[59] have recently examined the role of counterion charge and softness (polarizability) in controlling the shape of micelles on surfaces and have concluded that soft monoanions and dianions are more effective than hard anions in inducing growth from spherical to rodlike micelles. The laboratory of Romsted[42b] has argued that the ease of rod formation may depend, among others, on the stability of the hydrated tight ion pairs, which increases with the softness of the anion. According to the polarizability argument, *meta*- and *para*-fluorobenzoates are more polarizable than *ortho*-fluorobenzoates[42b,60] and should promote growth, whereas micelles in the presence of the relatively harder *ortho*-fluorobenzoate counterions should stay spherical. This expected behavior is matched by other experimental observations, which suggests that the polarizability of the anion may be of great importance in dictating the anions' average micellar position. With an increase in softness, the anions have a higher tendency to intercalate among the headgroups, which decreases headgroup repulsions and increases the likelihood of the anions to induce growth. This conclusion is also supported by our recent conductivity investigations of TTA^+ surfactants comicellized with *ortho*-bromobenzoates. These micelles form rods,[55] which is consistent with the fact that *ortho*-bromobenzoates are softer than *ortho*-fluorobenzoates.

The finding that TTA^+/*meta*- and *para*-fluorobenzoate micelles undergo sphere-to-rod transformations at the second cmc correlates with the cmc values and the hydrophobicity of the parent benzoic acids as is shown in Table 1. The data in the table, which lists among others the cmc and the log *P* values of fluorobenzoic acids and for comparative reasons also of toluic acids,[61] suggest that anions with the largest hydrophobicity values of the parent acids induce a change in micelle morphology. The *para*- and *meta*-substituted benzoic acids have larger hydrophobicity values than their parent *ortho*-substituted acids, which is in agreement with our experimental observation that TTA^+/*para*- and *meta*-fluorobenzoate micelles grow

(59) Subramanian, V.; Ducker, W. A. *Langmuir* **2000**, *16*, 4447−4454.

(60) Gronert, S. Private communication.

(61) Leo, A. *J. Chem. Soc., Perkin Trans. 2* **1983**, 825−838.

and form rodlike structures, whereas TTA^+ aggregates comicellized with *ortho*-fluorobenzoate remain spherical. We even like to speculate that micelles with incorporated anions that have hydrophobicity values for the parent acids larger than 2.0 promote growth, whereas those with values less than 2.0 do not. This hypothesis is based on our recent TTA^+/toluate investigations. Preliminary conductivity data of TTA^+/*meta- and para*-toluate micelles reveal a second cmc for these aggregates, which, as a marker of growth, indicates the transformation to rodlike micelles. For TTA^+/*ortho*-toluates, we postulate that these micelles stay spherical up to concentrations of about 20 times the cmc and then may start to grow, which is consistent with the hydrophobicity value of *ortho*-toluic acid being larger than 2.0. Whether a hydrophobicity value of 2.0 is indeed a threshold value for predicting growth for aggregates comicellized with *ortho*-, *meta*-, and *para*-substituted benzoate anions is under current investigation in our laboratories.

As an additional salient feature, the TTA^+/*ortho*-fluorobenzoate micelle studies allow us also to start addressing the importance of hydrogen bonding in promoting micellar growth. It has been suggested that an anion that forms hydrogen bonds is more likely to induce rod formation than an anion without hydrogen-bonding capabilities.[62] This is shown by studies of the most commonly investigated salicylate anion, which acts as hydrogen bond donor, stabilizes micelle formation, and promotes growth to rodlike micelles immediately after the onset of the cmc.[7−9,12−15] In contrast to salicylate, *ortho*-fluorobenzoate acts primarily as hydrogen bond acceptor and does not promote growth. This observation suggests either that an anion with hydrogen-bond donating properties will promote the transformation from spherical to rodlike micelles or that the favorable solvation of the hydrophilic OH substituent causes an ion, such as salicylate, to preferentially localize among the headgroups, where it can reduce effectively unfavorable headgroup repulsions. Current studies in our laboratory focus on hydrogen-bonding aspects.

Conclusions

The tandem approach of NMR chemical shift and conductivity data analyses exemplifies that this methodology provides a powerful tool for deducing the critical micelle concentration and for delineating micelle growth. The number of breakpoints observed in both the conductivity and NMR plots indicates that TTA^+/*ortho*-fluorobenzoate micelles remain roughly spherical over the large concentration range studied, whereas TTA^+/*meta*- and *para*-fluorobenzoates are gradually transformed from spherical to rodlike micelles at a surfactant concentration 10 times the cmc. The most significant findings of our studies can be summarized as follows: (i) The ^1H NMR spectra reveal two markers of growth at TTA^+/fluorobenzoate concentrations 10 times the cmc: the breakpoint in the graphs, in which the chemical shifts are plotted versus increasing or the inverse of increasing surfactant concentration, and the reversal of chemical shift direction of the resonances of the protons that strongly interact with the surfactant headgroups. (ii) The major factor inducing growth from spherical to rodlike micelles is provided by the ability of the counterions to reduce headgroup repulsions. The *meta*- and *para*-fluorobenzoates are very effective in performing this task, since they have the correct hydrophobicity/hydrophilicity balance to intercalate among the TTA^+ headgroups, thereby forming tight ion pairs. This intercalation reduces headgroup repulsions and allows for tighter packing, which initiates the transformation of spherical to rodlike micelles. (iii) The polarizability of the anion may be of great importance for inducing micelle growth, since it may dictate the anion's position and orientation at the micellar interface. Studies are currently under way in our laboratories to explore the importance of the polarizability of the counterion in promoting rod formation.

Experimental Section

Instrumentation. Conductivity data were recorded at 298 K on individually prepared samples with a 1062 Markson digital conductivity meter equipped with a platinum dip type cell, which was calibrated with standard KCl solutions.[63] The specific conductance values were reproducible to within 5 μS/cm. Surface tension measurements were recorded at room temperature on a Du Nouy tensiometer (CSC Scientific 70535) using a 5.992 cm circumference platinum ring. Proton NMR spectroscopy was performed on either a General Electric QE Plus 300 MHz spectrometer operating at 300.173 MHz or a BRUKER Avance DRX 300 MHz wide-bore spectrometer operating at 299.9200 MHz. ^{19}F and ^{13}C NMR spectroscopy studies were carried out on the Bruker instrument at frequencies of 282.1899 and 75.4149 MHz, respectively.

Materials. Tetradecyltrimethylammonium bromide (TTAB) (99%) was purchased from Aldrich Chemical Co. and used without further purification. Sodium dodecyl sulfate (SDS) (electrophoresis grade) was obtained from Ultra and used without further purification for the Epton two-phase titration.[64] For this titration, dichloromethane and a dual dye solution composed of 3,8-diamino-5-methyl-6-phenyl-phenanthridinium bromide (Aldrich) and Sulfan Blue {*N*-[4-[[4-(diethylamino)phenyl] (2,4-disulfophenyl)methylene]-22,5-cyclo-hexdien-1-ylidene] diethylammonium hydroxide} (Merck) dissolved in ethanol was used as purchased from British Drug House (BDH) Limited (product no. 19189). The NMR spectra were recorded in D_2O (99.8%), which was purchased from Aldrich or Cambridge Isotopes.

TTA^+/Fluorobenzoate Surfactant Preparation. The TTA^+/*ortho*-, *meta*-, and *para*-fluorobenzoate surfactants were prepared from a 80 mM TTAB stock solution by exchange of the bromide with hydroxide ions on an ion exchange column (J. T. Baker, Dowex 2-X8, 20−50 mesh). Aliquots of the TTAOH solutions, which were eluted from the column and analyzed by the Epton two-phase titration[64] to determine the TTA^+ concentration, were reacted with stoichiometric amounts of the corresponding *ortho*-, *meta*-, and *para*-fluorobenzoic acids (Aldrich Chemical Co.) in analogy to the procedure described by Lianos et al.[65] The solutions were allowed to react at 333 K for 20−30 min to yield the TTA^+/fluorobenzoate surfactants. The solutions were freeze-dried to isolate the solid surfactants. Surfactant stock solutions (75 mM) were prepared in distilled water and were quantified by a two-phase titration as described previously.[28]

Determination of the cmc Values, the Fractional Ionization Constant α, and the Onset of Aggregate Growth. The surface tension and conductivity measurements were performed as previously reported.[27,28] The Gibb's adsorption isotherm equation[66] was used to calculate the cmc values (Table 1) for all TTA^+/fluorobenzoates. The specific conductance was plotted versus increasing total surfactant concentration, and a linear regression analysis was used to determine the cmc's at 298 K and the onsets of micellar aggregate growth. The cmc values were taken from the intersection of the tangents drawn before and after the break in the graphs, where the conductivity is plotted versus total surfactant concentration (Figure 1). The

(62) Schick, M. J.; Fowkes, F. M. *J. Am. Chem. Soc.* **1957**, *61*, 1062−1068.

(63) Prue, P. R. In *The Table of Physical and Chemical Constants*, 14th ed.; Kaye, G. W. C., Laby, T. H., Eds.; Longman: New York, 1973; p 214.

(64) Schmitt, T. M. *Analysis of Surfactants*; Marcel Dekker: New York, 1992; pp 344−345.

(65) Lianos, P.; Zana, R. *J. Phys. Chem.* **1983**, *87*, 1289−1291.

(66) Rosen, M. J. In *Surfactants and Interfacial Phenomena*, 2nd ed.; Wiley-Interscience: New York, 1989; pp 65−66.

onsets of growth for the TTA^+/*meta*- and *para*-fluorobenzoate micelles were determined in an analogous fashion. To illustrate that TTA^+/*ortho*-fluorobenzoate micelles stay spherical over the concentration range studied, the data for this system are also graphed in Figure 1. The cmc's and the onset of growth were also deduced from the ^1H NMR spectra, in which the chemical shifts are plotted versus increasing or the inverse of increasing TTA^+/fluorobenzoate concentrations as described by Persson et al.[53] (Figure S3). The plots yielded straight lines with intersections at the inverse of the cmc and the onset of rodlike micelle formation. The cmc values are summarized in Table 1 together with the fractional ionization constants α, which were calculated using the Evan's equation[54] as previously reported.[27]

NMR Spectroscopy. The ^1H, ^{19}F, and ^{13}C NMR spectroscopy studies were carried out at a constant temperature of 298 K. Proton and carbon-13 chemical shifts were referenced to DSS (2,2-dimethyl-2-silapentane-5-sulfonate) for the aqueous (D_2O) solutions, in which the $-Si(CH_3)_3$ resonance frequency was set to 0.000 ppm. The chemical shifts are given with an accuracy of ±0.002 ppm for the Bruker and ±0.005 ppm for the QE spectrometer. The ^{19}F chemical shifts were recorded using a coaxial capillary insert with CCl_3F in $CDCl_3$ as the internal standard. The spectra were referenced to the ^{19}F signal of CCl_3F, which was set to 0.000 ppm. The ^1H, ^{13}C, and ^{19}F chemical shifts of the TTA^+/fluorobenzoate systems are listed in Tables 2−4.

^1H NMR Spectroscopy. The one-dimensional ^1H NMR spectra were acquired on either the Bruker Avance DRX or the QE-Plus spectrometer using the one-pulse sequences *zg* or *one pulse* available in the Bruker or General Electric pulse sequence library, respectively. The ^1H NMR spectra on the Bruker instrument were recorded with an inverse-detected multinuclear probe and the following acquisition parameters: 8−32 transients, a spectral width of 5708 Hz, a data size of 16 or 32K points, and a relaxation delay of 1.0 s to give an acquisition time of 1.36 or 2.87 s, respectively. The free induction decays (FIDs) were signal-averaged, apodized with a line-broadening factor of 0.1 Hz, Fourier transformed, phase corrected, and referenced. The ^1H NMR spectra on the QE-Plus spectrometer were recorded with a $^1H^{13}C$ dual probe using 64−1024 transients, a spectral width of 3000 Hz, and a relaxation delay of 1.0 s. The FIDs were signal-averaged, apodized with a line-broadening factor of 0.2 Hz, Fourier transformed, phase corrected, and referenced. To assign the ^1H NMR spectra of the TTA^+/fluorobenzoates, two-dimensional ^1H pulsed field gradient (PFG) COSY maps and ^{19}F-decoupled ^1H NMR spectra were acquired. The PFG COSY maps were recorded on the Bruker spectrometer using the pulsed field gradient sequence *COSYgp*, 128 data points in t_1 of 8 scans each over a spectral bandwidth of 897.99 Hz, and 512 data points in t_2. The data were processed with a sine function in F_1 and an exponential multiplication in F_2 and zero-filled to yield a final matrix of 1024 × 1024 data points. The fluorine-decoupled ^1H spectra were recorded with the pulse sequence *zgfhigqn* using a spectral width of 336.02 Hz, a data size of 1K, and a relaxation delay of 500 ms to give an acquisition time of 1.52 s. Depending on the TTA^+/fluorobenzoate concentrations, 128−1980 acquisitions were signal-averaged and apodized with a line-broadening factor of 0.3 Hz prior to Fourier transformation and phase correction.

^{13}C NMR Spectroscopy. The broadband-decoupled ^{13}C NMR spectra were acquired with a four-nuclei QNP probe with the one-pulse sequence *zgdc* (Bruker pulse sequence library, *WALTZ-16* decoupling). Typically, the spectra were recorded with a data size of 32K, a spectral width of 9578 Hz, and a relaxation delay of 1.0 s to give an acquisition time of 1.71 s. A minimum of 1280 transients was signal-averaged. The data were apodized with a line-broadening factor of 1.0 Hz prior to Fourier transformation and phase correction. The ^{13}C resonance assignments were confirmed by heteronuclear correlation (HETCOR) and multiple bond correlation (HMQC) spectroscopy. The HETCOR map was acquired with the *hxco* pulse sequence using 256 data points in F_1, a spectral width of 16556 Hz, and 1024 data points in F_2 with 8 acquisitions per t_1 increment. The time domain data were processed with an exponential multiplication in F_1 and a sine function in F_2 and zero-filled once in F_1 to yield a final matrix of 1024 × 512 data points. The HMQC data sets were acquired with the pulsed field gradient *inv4gp* pulse sequence using 128 data points in F_1 over a spectral width of 8098 Hz and 1024 data points in F_2 with 16 acquisitions per t_1 increment. The time domain data were processed with a sine function in F_1 and F_2 and zero-filled to a final matrix of 1024 × 1024 data points.

^{19}F NMR Spectroscopy. The proton-coupled ^{19}F NMR spectra were recorded with the pulse sequence *zg* (Bruker pulse sequence library), a bandwidth of 45351.5 Hz, a data size of 32K, and a relaxation delay of 1.0 s to give an acquisition time of 361 ms. Acquisitions (64−512) were signal-averaged and apodized with a line-broadening factor of 3.0 Hz prior to Fourier transformation and phase correction.

Acknowledgment. This investigation was in part supported by a *Research Infrastructure in Minority Institutions* (RIMI) award from the National Center for Research Resources with funding from the Office of Research on Minority Health, National Institutes of Health No. 5 P20 RR11805; a grant from the National Institutes of Health, MBRS SCORE Program (No. S06 GM52588); and grants from the National Science Foundation (CHE-9816356), the Camille & Henry Dreyfus Foundation, and Research Corporation (all to U.S.). Supports from the Department of Chemistry & Biochemistry and the College of Science & Engineering at San Francisco State University (SFSU) and the Department of Chemistry at Saint Mary's College of California are gratefully acknowledged. The Department of Chemistry & Biochemistry at SFSU acknowledges grants from the NIH (RR 02684) and NSF (DMB-8516065, DUE-9451624 U.S.) for the purchase of the NMR spectrometers.

Supporting Information Available: The ^{19}F-decoupled ^1H spectra of all micellar systems, the PFG COSY maps of TTA^+/*ortho*- and *meta*-fluorobenzoates, and an example of the determination of the cmc and second cmc values from the intersections of the regression lines in the ^1H NMR inverse plots. This material is available free of charge via the Internet at http://pubs.acs.org.

LA0109765